Stability and bifurcation analysis of a Van der Pol–Duffing oscillator with a nonlinear tuned vibration absorber

Giuseppe Habib and Gaetan Kerschen*
Department of Aerospace and Mechanical Engineering, University of Liege, Liege, Belgium

Summary. The Van der Pol (VdP) oscillator is a paradigmatic model for description of self-excited oscillations, which are of practical interest in many engineering applications. In this paper the dynamics of a VdP–Duffing (VdPD) oscillator with an attached nonlinear tuned vibration absorber (NLTVA) is considered; the NLTVA has both linear and nonlinear restoring force terms. In the first part of this work, the stability of the trivial solution of the system is investigated, following results of previous works. The analysis allows to define an optimal tuning rule for the linear parameters of the absorber, which substantially enlarges the domain of safe operation of the primary system. In this case, the system loses stability through a double Hopf bifurcation. In the second part of this work, the bifurcations occurring at the loss of stability are analytically investigated, using the technique of the center manifold reduction and transformation to normal form. The obtained results show the effects of the nonlinear parameter of the absorber, which, in turn, allows to define its optimal value in order to avoid subcriticality and reduce the amplitude of self-excited oscillations.

Introduction

Limit cycle oscillations (LCO) occur in many mechanical systems and they are often a source of danger [1]. Aircraft wings are a typical example of systems generating dangerous LCO [2]. Nowadays there is a trend to design lighter and more flexible aerospace, but also civil engineering structures, which then become more prone to LCOs.
Among the passive systems to mitigate LCOs, the addition of a relatively small mass to the host system, attached through a linear spring and a damper (linear tuned vibration absorber, LTVA), has been widely studied in the literature [3]-[8]. References [5] and [6] provide simple rules to properly tune the parameter of the LTVA, while references [7] and [8] study the post-bifurcation behavior of the system, which loses stability through a simple Hopf bifurcation [7] or a double Hopf (DH) bifurcation [7, 8]. In most of the these works, the system under investigation is a classical Van der Pol (VdP) oscillator.
Recently, the nonlinear energy sink (NES), an absorber with an essentially nonlinear spring (i.e., a nonlinearizable nonlinearity), received growing attention [9]-[11]. Such a system allows to transfer the energy from the primary system to the absorber mass in a process called targeted energy transfer (TET). Its effectiveness for externally-excited systems has been widely investigated in several cases [9].
The difference between the LTVA and NES is essential. The use of a linear spring allows to enlarge the stable region of the trivial solution of the primary system for larger values of the bifurcation parameter (i.e., a negative damping coefficient in the case of the VdP oscillator or the flow speed for aeroelastic instability), as shown in [7]. Conversely, the addition of an essentially nonlinear system leaves almost unchanged the stable region, but it can sensibly mitigate the LCO in the post-bifurcation behavior of the system [12].
The main idea of this work is to combine these two positive effects and to develop an absorber, termed the nonlinear tuned vibration absorber (NLTVA), that possesses a spring with both linear and nonlinear characteristics. A similar system was already studied in [13], where the nonlinearity was brought by damping effects. The results obtained therein showed that nonlinear damping decreases the effectiveness of the LTVA, but it can also improve the post-bifurcation behavior of the system if the underlying linear system is slightly detuned.
The primary system considered herein is an extended version of the typical VdP oscillator [14], which is a paradigmatic model for description of self-excited oscillations. Adding a cubic nonlinearity to the primary system, it is possible to obtain a large variation of the LCO frequency [12], which allows to give more generality to our investigation. This modified system is usually referred to as Van der Pol–Duffing (VdPD) oscillator [15].
In the first part of this work, we will retrace the stability analysis of the trivial solutions of the two-degree-of-freedom (DoF) system (VdPD oscillator with an attached NLTVA), already exhaustively solved in [7]. In the second part, the bifurcations occurring at the loss of stability will be analytically investigated. This will allow us to (i) identify the effects of the nonlinear spring of the NLTVA, (ii) define its optimal value in order to avoid subcriticality and (iii) minimize the response in the post-bifurcation regime.

Mathematical model and stability analysis

We consider a VdPD oscillator, with a lumped mass attached through a linear damper and a spring with linear and cubic components. The equations of motion of the system under study are

$$m_1 q_1'' + c_1 \left(q_1^2 - 1\right) q_1' + k_1 q_1 + k_{nl1} q_1^3 + c_2 \left(q_1' - q_2'\right) + k_2 \left(q_1 - q_2\right) + k_{nl2} \left(q_1 - q_2\right)^3 = 0 \tag{1}$$

$$m_2 q_2'' + c_2 \left(q_2' - q_1'\right) + k_2 \left(q_2 - q_1\right) + k_{nl2} \left(q_2 - q_1\right)^3 = 0 \tag{2}$$

*The authors G. Habib and G. Kerschen would like to acknowledge the financial support of the European Union (ERC Starting Grant NoVib-307265).

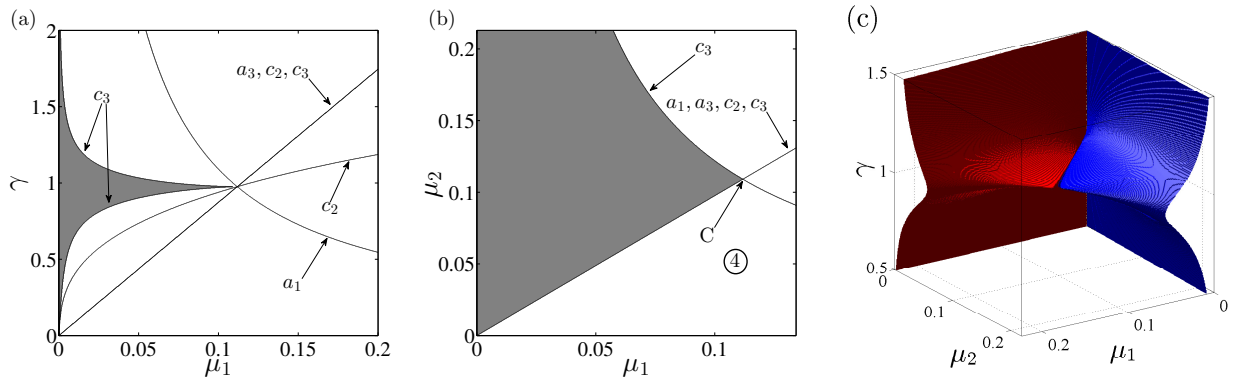

Figure 1: Stability chart in the space μ_1, γ (a) and μ_1, μ_2 (b). Shaded area: stable, white region: unstable. Encircled number 4 indicates a region with 4 complex conjugate eigenvalues in pairs with positive real part. In the figure $\varepsilon = 0.05$; (a): $\mu_2 = 1/2\sqrt{\varepsilon/(1+\varepsilon)}$; (b): $\gamma = 1/\sqrt{1+\varepsilon}$. (c): stability chart in the μ_1, μ_2, γ space; the blue surface indicates the stability border, while the red surface indicates the border of the area with four eigenvalues with positive real part.

which, introducing the dimensionless time $\tau = t/\omega_{n1}$ and the variable transformation $q_d = q_1 - q_2$, can be rewritten in matrix form as

$$\begin{bmatrix} 1 & 0 \\ 0 & 1 \end{bmatrix} \begin{bmatrix} \ddot{q}_1 \\ \ddot{q}_d \end{bmatrix} + \begin{bmatrix} -2\mu_1 & 2\mu_2\gamma\varepsilon \\ -2\mu_1 & 2\mu_2\gamma\,(1+\varepsilon) \end{bmatrix} \begin{bmatrix} \dot{q}_1 \\ \dot{q}_d \end{bmatrix} + \begin{bmatrix} 1 & \gamma^2\varepsilon \\ 1 & \gamma^2\,(1+\varepsilon) \end{bmatrix} \begin{bmatrix} q_1 \\ q_d \end{bmatrix} + \begin{bmatrix} 2\mu_1 q_1^2\dot{q}_1 + \alpha_3 q_1^3 + \beta_3\varepsilon q_d^3 \\ 2\mu_1 q_1^2\dot{q}_1 + \alpha_3 q_1^3 + \beta_3\,(1+\varepsilon)\,q_d^3 \end{bmatrix} = \begin{bmatrix} 0 \\ 0 \end{bmatrix} \tag{3}$$

or in compact form $\mathbf{M}\ddot{\mathbf{q}} + \mathbf{C}\dot{\mathbf{q}} + \mathbf{K}\mathbf{q} + \mathbf{b} = \mathbf{0}$, where $\mathbf{b}$ includes all nonlinear terms, $\varepsilon = m_2/m_1$, $2\mu_1 = c_1/(m_1\omega_{n1})$, $2\mu_2 = c_2/(m_2\omega_{n2})$, $\omega_{n1}^2 = k_1/m_1$, $\omega_{n2}^2 = k_2/m_2$, $\gamma = \omega_{n2}/\omega_{n1}$, $\alpha_3 = k_{nl1}/(m_1\omega_{n1}^2)$ and $\beta_3 = k_{nl2}/(m_2\omega_{n1}^2)$.
The trivial solution of Eq. (3) is asymptotically stable if and only if the poles of the characteristic polynomial of the linear part of the system have negative real part. The characteristic polynomial is given by $\det\left(z^2\mathbf{M}\ddot{\mathbf{q}} + z\mathbf{C}\dot{\mathbf{q}} + \mathbf{K}\mathbf{q}\right) = 0$, i.e.

$$z^4 + z^3 2\left((\varepsilon+1)\gamma\mu_2 - \mu_1\right) + z^2\left((\varepsilon+1)\gamma^2 - 4\gamma\mu_1\mu_2 + 1\right) + z2\gamma(\mu_2 - \gamma\mu_1) + \gamma^2 = 0 \tag{4}$$

or $a_4 z^4 + a_3 z^3 + a_2 z^2 + a_1 z + a_0 = 0$. According to the Routh-Hurwitz criterion, the characteristic polynomial has poles with negative real parts if and only if the coefficients $a_i > 0$, $i = 1, ..., 4$, $c_2 = (a_3 a_2 - a_4 a_1)/a_3 > 0$ and $c_3 = c_2 a_1 - a_3 a_0 > 0$.
Considering the values of these coefficients, it is possible to define the stability chart of the system. The aim of this analysis is to obtain a set of parameters such that the value of μ_1 that gives stability is maximized. Figure 1 (a) shows a section of the stability chart in the μ_1, γ space for $\mu_2 = 1/2\sqrt{\varepsilon/(1+\varepsilon)} = 0.1091$. The curves $a_3 = 0$ and $a_1 = 0$ intersect at $\gamma = 1/\sqrt{1+\varepsilon}$. Substituting this value in $c_3 = 0$, it can be easily verified that the stable region is maximized if $\mu_2 = 1/2\sqrt{\varepsilon/(1+\varepsilon)}$, which is therefore the optimal value of μ_2.
Figure 1 (b) shows a section of the stability chart in the μ_1, μ_2 space for $\gamma = 1/\sqrt{1+\varepsilon} = 0.9759$. Fig. 1 (c) confirms the obtained results for optimal tuning of the absorber, i.e. for $\gamma = 1/\sqrt{1+\varepsilon}$ the stable region is maximized, while a small detuning of γ sensibly reduce the stable area.
The coordinates of point C in Fig. 1 (b) are $\mathrm{C} = \left(\sqrt{\varepsilon}/2, 1/2\sqrt{\varepsilon/\,(1+\varepsilon)}\right)$ and, according to our calculations, the optimal values of the absorber parameters are

$$\gamma_{\text{opt}} = \frac{1}{\sqrt{1+\varepsilon}} \quad \text{and} \quad \mu_{2\text{opt}} = \frac{1}{2}\sqrt{\frac{\varepsilon}{1+\varepsilon}} \tag{5}$$

and, if those equations are satisfied, the maximal value of μ_1 in order to have stability is $\mu_{1\max} = \sqrt{\varepsilon}/2$. If γ is properly tuned, the stability region is delimited by the curves $\mu_1 = \varepsilon/\left(4\mu_2\sqrt{1+\varepsilon}\right)$ on the top and $\mu_1 = \mu_2\sqrt{1+\varepsilon}$ on the bottom.

Bifurcation analysis

Analyzing directly the poles of Eq. (4), it is possible to identify the bifurcations occurring at the loss of stability. Although not indicated in the figures, from our analysis it appears that at the loss of stability one or two couples of complex conjugate eigenvalues leave the half-plane of negative real values, which corresponds respectively to a Hopf and to a DH bifurcation. The area with four complex conjugate eigenvalues with positive real parts is marked with the encircled number 4 in Fig. 1 (b) and in red in Fig. 1 (c).
The existence of subcritical bifurcations would compromise the robustness of the trivial solution within the stable region, particularly in the vicinity of the stability border. Thus, the narrow strip in correspondence of the optimal tuning (Fig.

1) appears to be critical in this sense. Furthermore, if μ_2 is smaller than the optimal value, at the loss of stability a DH bifurcation is taking place, which probably has a very involved scenario and could generate quasiperiodic solutions.
It is also remarkable that a locus of DH bifurcations can be exactly defined (line from 0 to C in Fig. 1 (b)). Its equations are

$$\begin{cases} \mu_1 = \mu_2\sqrt{1+\epsilon} \\ \gamma = \frac{1}{\sqrt{1+\varepsilon}} \end{cases} \tag{6}$$

with $0 < \mu_1 < \sqrt{\varepsilon}/2$.
A detailed investigation of the bifurcations occurring at the loss of stability, would allow to define the optimal choice of the nonlinear parameters of the NLTVA, in order to reduce the amplitude of the generated vibrations and to have supercritical bifurcations, rather than subcritical.
In order to study the most important bifurcations of the system, we first transform it into a system of first order differential equations

$$\begin{bmatrix} \dot{x}_1 \\ \dot{x}_2 \\ \dot{x}_3 \\ \dot{x}_4 \end{bmatrix} = \begin{bmatrix} 0 & 1 & 0 & 0 \\ -1 & 2\mu_1 & -\gamma^2\varepsilon & -2\mu_2\gamma\varepsilon \\ 0 & 0 & 0 & 1 \\ -1 & 2\mu_1 & -\gamma^2(1+\varepsilon) & -2\mu_2\gamma(1+\varepsilon) \end{bmatrix} \begin{bmatrix} x_1 \\ x_2 \\ x_3 \\ x_4 \end{bmatrix} + \begin{bmatrix} 0 \\ -2\mu_1 x_1^2 x_2 - \alpha_3 x_1^3 - \beta_3\varepsilon x_3^3 \\ 0 \\ -2\mu_1 x_1^2 x_2 - \alpha_3 x_1^3 - \beta_3(1+\varepsilon) x_3^3 \end{bmatrix} \tag{7}$$

or in compact form $\dot{\mathbf{x}} = \mathbf{A}\mathbf{x} + \mathbf{b}$.

Single Hopf bifurcations

Except along line OC in Fig. 1 (b), the system loses stability through single Hopf bifurcations. In the following, we perform a local analysis of these bifurcations in order to define their nature, i.e. if they are subcritical or supercritical, and the effects of the nonlinear terms.
In correspondence of the loss of stability, $\mathbf{A}$ has a couple of complex conjugate eigenvalues with zero real part and two other eigenvalues with negative real parts. We call $\lambda_{1,2} = k_1 \pm i\omega_1$ the eigenvalues with zero real part and λ_3 and λ_4 the other two.
Defining a transformation matrix through the eigenvectors of $\mathbf{A}$, we can decouple the linear part of the system. Then, applying a center manifold reduction it is possible to eliminate the variable not related to the bifurcation, reducing the dimension of the system without affecting the local dynamics. Performing then a transformation in complex form, a near identity transformation and a transformation in polar coordinates, we obtain the normal form of a Hopf bifurcation, i.e.

$$\dot{r} = k_1 r + \delta r^3. \tag{8}$$

Eq. (8) has solutions $r_0 = 0$ and $r^* = \sqrt{-k_1/\delta}$. The bifurcation is supercritical if $\delta < 0$ and subcritical if $\delta > 0$.
Considering the order of the terms, it can be defined that

$$\delta = \delta_0(\varepsilon, \gamma, \mu_1, \mu_2) + \delta_{\alpha_3}(\varepsilon, \gamma, \mu_1, \mu_2)\alpha_3 + \delta_{\beta_3}(\varepsilon, \gamma, \mu_1, \mu_2)\beta_3, \tag{9}$$

which is also confirmed by calculation. This means that δ varies linearly with respect to α_3 and β_3.

Optimization

Negative values of δ_0 indicate that the bifurcation is supercritical if $\alpha_3 = \beta_3 = 0$, while if $\delta_0 > 0$ it is subcritical under the same conditions. Similarly, if $\delta_{\alpha_3} < 0\,(> 0)$ positive values of α_3 decrease (increase) the value of δ, facilitating supercritical (subcritical) properties of the bifurcation. The same applies for δ_{β_3} and β_3. Generally, in real applications, the value of α_3 is given, while the value of β_3 can be chosen properly tuning the absorber. In most applications, the aim of the absorber is to make the bifurcations supercritical and to reduce the oscillation amplitude in the post-bifurcation regime. Large negative values of δ correspond to low oscillation amplitudes, however, high values of the nonlinear terms might cause other nonlinear phenomena overlooked by this local analysis. The amplitude of oscillation is also influenced by the real part of λ_1, which is determined uniquely by the linear terms.
Applying the outlined procedure along the significant area of the stability boundary we obtain the diagrams in Fig. 2. We remind that on the line going from $\mu_1 = 0$, $\mu_2 = 0$ and $\gamma = \gamma_{\text{opt}}$ until point C, DH bifurcations take place, thus this analysis is insufficient to describe their local dynamics. C corresponds to the point of loss of stability for optimal values of γ and μ_2.
Fig. 2 (a) shows that δ_0 is always negative along the stability border, thus a pure VdP oscillator with a linear absorber undergoes supercritical Hopf bifurcations only. Furthermore, its absolute value is much larger in the vicinity of point C (for $\mu_2 > \mu_{2\text{opt}}$) than on the rest of the stability border, which indicates a better post-bifurcation behavior. Far from the area influenced by the absorber, where the loss of stability occurs for low values of μ_1, δ_0 is close to zero, which is consistent to the fact that, in absence of the absorber, $\delta = 0$ if there is no Duffing term.
Fig. 2 (b) shows the value of δ_{α_3}. It goes from positive to negative values, indicating an opposite influence on the bifurcation depending on the position of the loss of stability. Comparing the two views of the figure (*top* and *bottom*) it is visible a sort of symmetric behavior. Furthermore, close to point C the absolute value of δ_{α_3} is much larger than far from

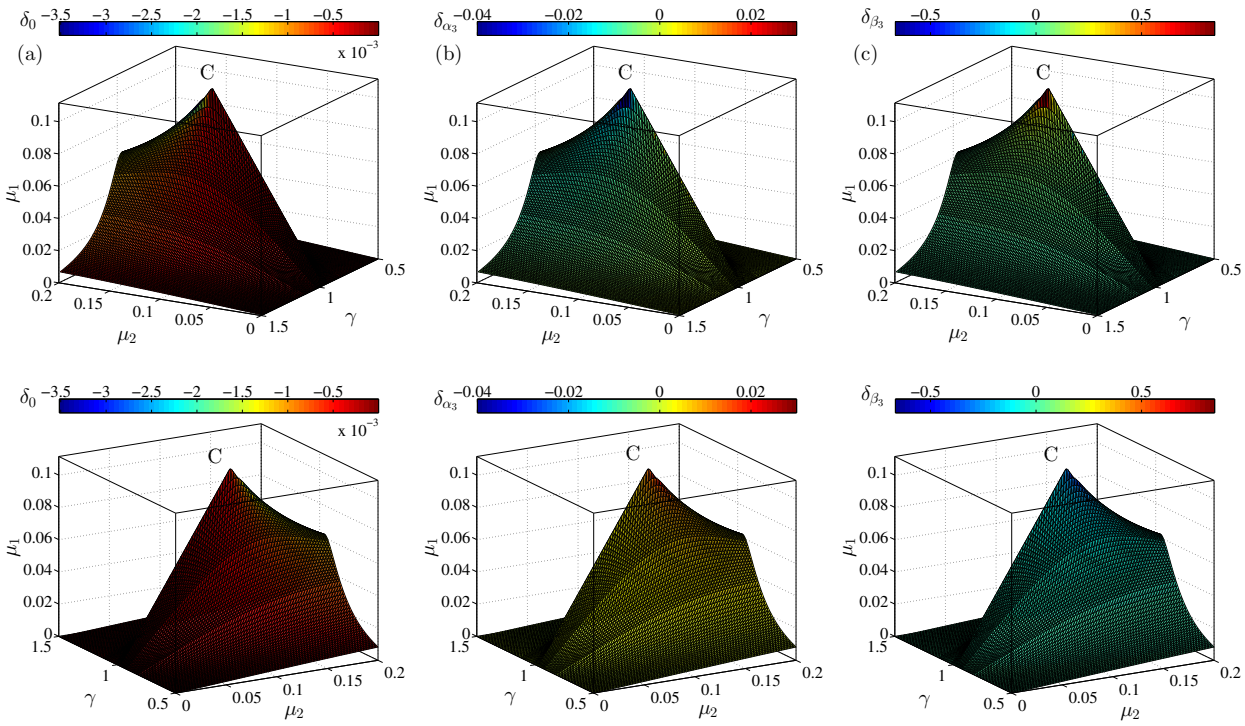

Figure 2: The surface correspond to the stability border in the μ_1, μ_2, γ space. The color indicates the value of δ_0 (a), δ_{α_3} (b) and δ_{β_3} (c). In the figure $\varepsilon = 0.05$.

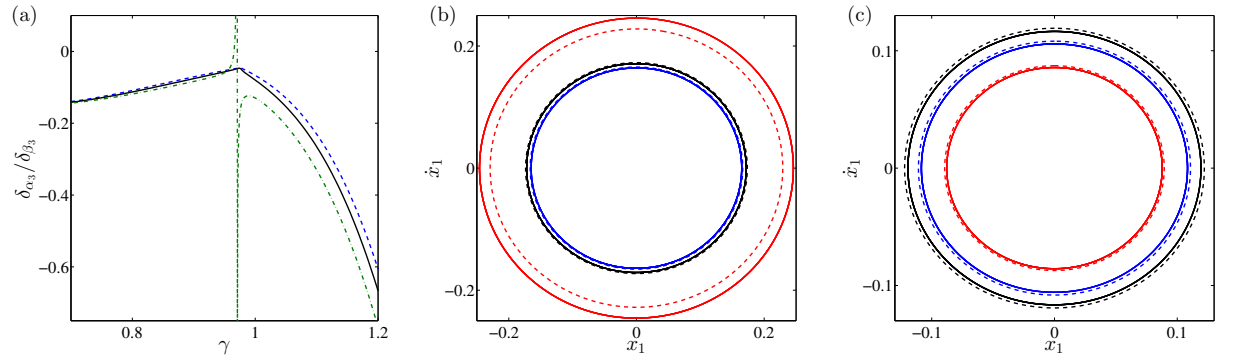

Figure 3: (a): trend of $\delta_{\alpha_3}/\delta_{\beta_3}$ as a function of γ for fixed values of μ_2 and $\varepsilon = 0.05$; solid black lines: $\mu_2 = \mu_{2\text{opt}} = 0.1091$, dashed blue lines: $\mu_2 = 0.07$, dash-dotted green lines: $\mu_2 = 0.13$. (b), (c): projections of the stable periodic attractor for different parameter values, $\varepsilon = 0.05$ and $\mu_2 = \mu_{2\text{opt}} = 0.1091$. (b): $\gamma = \gamma_{\text{opt}} = 0.9759$, $\mu_1 = 0.102$; (c): $\gamma = 0.9721$, $\mu_1 = 0.103$. Black: , $\alpha_3 = 0$, $\beta_3 = 0$; red: $\alpha_3 = 0.05$, $\beta_3 = 0$; blue: $\alpha_3 = 0.05$, $\beta_3 = 0.0025$. Dashed lines: analytical results, solid lines: numerical results.

it, which indicates that α_3 has a strong influence on the bifurcation behavior if the linear parameters of the absorber are correctly tuned. In addition, the fact that it goes from positive to negative values in a small region makes it very difficult to predict its effect. Fig. 2 (c) shows variations of δ_{β_3} along the stability border. The trend of δ_{β_3} is qualitatively similar to that of δ_{α_3}, but with opposite sign and a higher order of magnitude. This means that it is hard to reliably predict the effects of β_3 as well.

Considering a given primary system with a specific Duffing coefficient α_3, it is possible to properly tune the linear parameters in order to maximize the stable range of μ_1. After this optimization, the system will lose stability in the vicinity of point C. Due to unavoidable uncertainty it is not possible to define exactly the point of loss of stability. Therefore, it is troublesome to optimize β_3 such that δ is kept negative (to avoid subcriticality) and minimized (to decrease vibration amplitudes). However, the fact that δ_{α_3} and δ_{β_3} have similar trends, suggests that there might exist a general rule for tuning β_3 depending on α_3, in order to avoid subcriticalities.

Figure 3 (a) shows the ratio $\delta_{\alpha_3}/\delta_{\beta_3}$ for variations of γ for different values of μ_2. This figure exhibits that, in the relevant area in the case of accurate tuning of the linear terms, $\delta_{\alpha_3}/\delta_{\beta_3}$ is always negative and it varies in a relatively small range. Considering a crude approximation of $\delta_{\alpha_3}/\delta_{\beta_3} \approx -0.05$, we have that, setting $\beta_3 \approx 0.05\alpha_3$, the eventually detrimental effect of α_3 is compensated by β_3. An exact knowledge of all the parameter values would allow a much better tuning, but this would not be robust with respect to system uncertainties.

The dash-dotted green curve in Fig. 3(a) goes to infinity in correspondence of the change of sign of δ_{β_3}. Although this

appears as a failure of the previous statement because of the large variation of $\delta_{\alpha_3}/\delta_{\beta_3}$, since in that point $\delta_{\beta_3} \approx 0$ the effect of β_3 is anyway negligible (and in most of cases the effect of α_3 as well, since they go to zero almost together), thus a mistuning of β_3 has no detrimental effects. The other curves in the figure does not go to infinity, since δ_{α_3} and δ_{β_3} change sign for the same value of γ.
Figures 3 (b) and (c) show the periodic attractor, generated by the Hopf bifurcation, for different parameter values. All the curves in Fig. 3 (b) refer to the same parameter values for the linear part; the same, with a different value of γ, applies in Fig. 3 (c). If the system under study would refer to a real case, it would be hard to predict which of the two attractors is generated at the loss of stability, since their linear parts are only slightly different. The black lines refer to $\alpha_3 = \beta_3 = 0$. The red lines show that positive values of α_3 have opposite effects in the two cases: in one case the amplitude of the attractor increases, in the other it decreases. Confirming our predictions, the blue lines shows that a correct value of β_3 can compensate and nullify the effect of α_3, either if it is detrimental (Fig. 3 (b)) or if it is advantageous (Fig. 3 (c)). In this case $\beta_3 = 0.05\alpha_3$, since $\delta_{\alpha_3}/\delta_{\beta_3} \approx -0.05$. In the figure, the matching between the numerical and the analytical results confirms the validity of the procedure.

Double Hopf bifurcation

In order to have a clearer picture of the local post-bifurcation behavior, we perform a local analysis of the DH bifurcations occurring on line OC in Fig. 1 (b), due to the intersection of two loci of single Hopf bifurcations. The characteristic polynomial of $\mathbf{A}$ is the same as the one in Eq. (4), thus, on the line OC, $\mathbf{A}$ has two couples of complex conjugate eigenvalues with zero real part.
We call the eigenvalues $\lambda_1, \lambda_2, \lambda_3, \lambda_4$, where $\lambda_1 = \bar{\lambda}_2$ and $\lambda_3 = \bar{\lambda}_4$; $\lambda_{1,2} = k_1 \pm i\omega_1$ and $\lambda_{3,4} = k_2 \pm i\omega_2$. Applying a procedure similar to that used for the single Hopf bifurcation, we transform the system into its normal form, i.e.

$$\dot{r}_1 = r_1\left(k_1 + p_{11}r_1^2 + p_{12}r_2^2\right) \tag{10}$$

$$\dot{r}_2 = r_2\left(k_2 + p_{21}r_1^2 + p_{22}r_2^2\right). \tag{11}$$

For more details on this involved passages see [17]. The complete normal form of a DH bifurcation includes also fifth order terms, but they can be neglected for the dynamics encountered in this work.

Analysis of the normal form and bifurcation diagrams

Equations (10)-(11) are an amplitude system, whose solutions are directly connected to those of the original system. It has four types of fixed point solutions, namely: trivial solutions $(0,0)$, semi-trivial solutions $(\tilde{r}_1, 0)$ or $(0, \tilde{r}_2)$ and non-trivial solutions (r_1^*, r_2^*). The type of solutions existing in the vicinity of the bifurcation depends only on the real part of the eigenvalues, k_1 and k_2, since p_{11}, p_{12}, p_{21} and p_{22} can be considered constant for a local analysis.
The trivial solution $(0,0)$ exists for any value of k_1 and k_2, but it is stable if and only if $k_1 < 0$ and $k_2 < 0$. The existence and stability of the trivial solution were already studied in the stability analysis.
The semi-trivial solution $(\tilde{r}_1, 0)$, where $\tilde{r}_1 = \sqrt{-k_1/p_{11}}$, exists for $k_1/p_{11} < 0$ and it is stable if and only if $k_1 > 0$ and $k_1 > k_2 p_{21}/p_{11}$. Similarly, the semi-trivial solution $(0, \tilde{r}_2)$, where $\tilde{r}_2 = \sqrt{-k_2/p_{22}}$, exists for $k_2/p_{22} < 0$ and it is stable if and only if $k_2 > 0$ and $k_2 > k_1 p_{12}/p_{22}$. They correspond to two periodic solutions of the original system with frequency approximately ω_1 and ω_2, respectively, and they are generated by Hopf bifurcations of the trivial solution.
The non-trivial solution (r_1^*, r_2^*), where $r_1^* = \sqrt{(k_1 p_{22} - k_2 p_{12})/p^*}$ and $r_2^* = \sqrt{(k_2 p_{11} - k_1 p_{21})/p^*}$, $p^* = p_{12}p_{21} - p_{11}p_{22}$, exists if and only if r_1^* and r_2^* are real. It is generated by secondary Hopf bifurcations of a branch of periodic solutions and it corresponds to a quasiperiodic solution of the original system, with the two frequencies of oscillation being approximately ω_1 and ω_2.
If $p_{11} < 0$ and $p_{22} < 0$, the two branches of single Hopf bifurcations are both supercritical. Furthermore, if also $p_{12} < 0$, $p_{21} < 0$ and $p^* < 0$, there are no solutions (identified by this local analysis) different from the trivial one, within the stable region, which may involve larger attractors. This is the most desirable scenario in real applications of the NLTVA.
First, we consider the case with $\beta_3 = 0$, i.e. a linear tuned vibration absorber. In most cases, along the full locus of DH bifurcations, if $|\alpha_3|$ is small, we have the convenient case of $p_{11} < 0$, $p_{22} < 0$, $p_{12} < 0$, $p_{21} < 0$ and $p^* < 0$. A typical bifurcation chart for this case is shown in Fig. 4 (a) for $\mu_2 = 0.9\mu_{2\text{opt}}$ and $\alpha_3 = 0.01$.
Considering the bifurcation chart in Fig. 4, the periodic solution $(\tilde{r}_1, 0)$ exists in regions B, C, D and E, and it is stable in B, C and D. The other periodic solution $(0, \tilde{r}_2)$ exists in C, D, E and F, being stable in D, E and F. While the quasiperiodic solution (r_1^*, r_2^*) exists only in region D and it is unstable of saddle type. In Fig. 4 (b) a bifurcation diagram in the vicinity of a DH bifurcation is represented. Besides the perfect agreement between numerical and analytical results, the figure shows the region of coexistence of the two periodic solutions with the unstable quasiperiodic solution.
In Fig. 4 (c) the poincaré maps of the quasiperiodic solution, obtained numerically and analytically, are compared. The numerical result is fuzzy since the solution is unstable, so it diverges from it, however, the matching with the analytical predicted curve is excellent.

Optimization and tuning rule

In order to have a better insight into the effects of α_3 and β_3 on the DH bifurcations, we analyze the values of p_{11}, p_{12}, p_{21} and p_{22}, which can be expressed as $p_{ij} = p_{ij,0} + p_{ij,\alpha_3}\alpha_3 + p_{ij,\beta_3}\beta_3$, analogously to δ in Eq. (9). Following the procedure outlined in the previous section, we notice that $p_{ij,\alpha_3}/p_{ij,\beta_3} = -\varepsilon/(1+\varepsilon)^2$. Interestingly, this ratio is valid

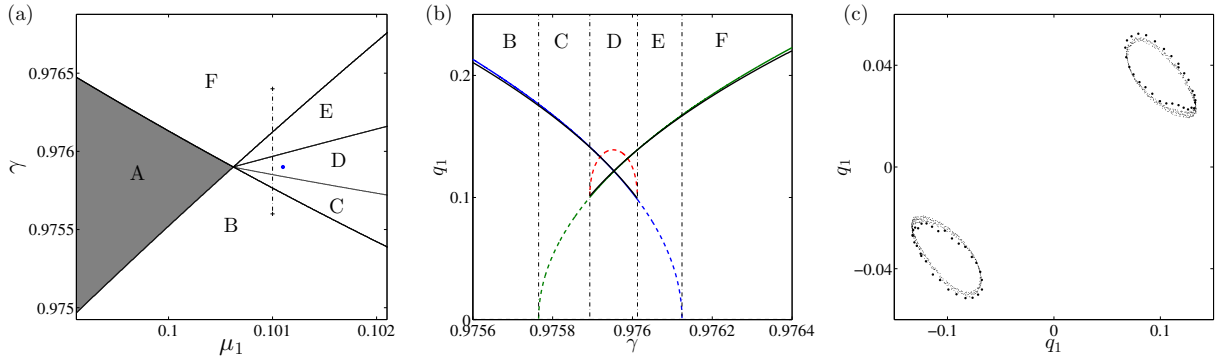

Figure 4: (a): bifurcation chart in the space $\mu_1\gamma$. Shaded area: stable, clear area: unstable. Letters from A to F indicates region with different behaviour. In the figure $\varepsilon = 0.05$, $\mu_2 = 0.9\mu_{2\text{opt}} = 0.0982$, $\alpha_3 = 0.01$ and $\beta_3 = 0$. The thin dash-dotted line refers to the paths followed by the bifurcation diagram in (b). (b): bifurcation diagram; (c): comparison of the poincaré maps of the analytical and of the numerical solutions in the point marked in blue in (a).

along the whole line OC and for all the coefficients. The practical consequence of this result is that, if $\beta_3 = \varepsilon/(1+\varepsilon)^2\alpha_3$, the effect of α_3 is locally entirely compensated by β_3. This tuning rule is valid, although approximated, also when the system undergoes single Hopf bifurcation. Its effectiveness is confirmed by the numerical and analytical plots in Fig. 4 (c).

The ratio $-\left(\mathrm{d}k_1/\mathrm{d}\mu_1\right)/\delta$ along the stability boundary is locally proportional to the amplitude of the LCO after stability loss. Although it is not shown here, our analysis evidences that it is close to a minimum in the case of optimal tuning of the linear and nonlinear parameters of the absorber. Furthermore, small detuning of the absorber parameters has slight effect on it, which guarantees robustness with respect to parameter uncertainties.

Discussion and conclusions

The objective of this study is to passively suppress the limit cycle oscillations of a VdPD oscillator using a NLTVA possessing both linear and nonlinear springs and a linear damper. The linear spring and damper are designed to sensibly enlarge the safe domain of operation of the VdPD oscillator, i.e., the domain where limit cycle oscillations are absent. The nonlinear spring is then determined to ensure supercriticality of the postbifurcation behavior, a feature of practical importance. Through a detailed analytical investigation of the bifurcations occurring at the loss of stability of the trivial solution, this latter feature of the NLTVA was attributed to the compensation of the nonlinear dynamics of the Van der Pol-Duffing oscillator by the nonlinear component of the absorber. Specifically, in the case of optimal tuning of the linear spring and damper, a simple closed form formula for the nonlinear spring was derived for a perfect compensation. Because all the results described in the present study are valid locally, our future research efforts will be geared toward a global analysis of the dynamics of the coupled system.

References

[1] Griffin O.M., Skop R.A. (1973) The vortex-excited resonant vibrations of circular cylinders. *J. Sound Vib.* **27**:235-249.

[2] Lee B.H.K., Jiang L.Y., Wong Y.S. (1999) Flutter of an airfoil with a cubic restoring force. *J. Fluid Struc.* **13**(1):75-101.

[3] Mansour W.M. (1972) Quenching of limit cycles of a van der Pol oscillator. *J. Sound Vib.* **25**(3):395-405.

[4] Tondl A. (1975) Quenching of self-excited vibrations equilibrium aspects. *J. Sound Vib.* **42**(2):251-260.

[5] Rowbottom M.D. (1981) The optimization of mechanical dampers to control self-excited galloping oscillations. *J. Sound Vib.* **75**(4):559-576.

[6] Fujino Y., Abe M. (1993) Design formulas for tuned mass dampers based on a perturbation technique. *Earth Eng. Struct. Dyn.* **22**:833-854.

[7] Gattulli V., Di Fabio F., Luongo, A. (2001) Simple and double Hopf bifurcations in aeroelastic oscillators with tuned mass dampers, *J. Franklin Inst.* **338**:187-201.

[8] Gattulli V., Di Fabio F., Luongo A. (2003) One to one resonant double hopf bifurcation in aeroelastic oscillators with tuned mass dampers *J. Sound Vib.* **262**:201-217.

[9] Vakakis A.F., Gendelman O.V., Kerschen G., Bergman L.A., McFarland M.D., Lee Y.S. (2009) Nonlinear Target Energy Transfer in Mechanical and Structural Systems. Springer.

[10] Gendelman O.V., Bar T. (2010) Bifurcations of self-excitation regimes in a Van der Pol oscillator with a nonlinear energy sink. *Physica D* **239**:220-229.

[11] Guo H.L., Chen Y.S. Yang T.Z. (2013) Limit cycle oscillation suppression of 2-DOF airfoil using nonlinear energy sink. *Appl. Math. and Mech.* **34**(10):1277-1290.

[12] Domany E., Gendelman O.V. (2013) Dynamic responses and mitigation of limit cycle oscillations in Van der Pol–Duffing oscillator with nonlinear energy sink. *J. Sound Vib.* **332**(21):5489-5507.

[13] Gattulli V., Di Fabio F., Luongo A. (2004) Nonlinear Tuned Mass Damper for self-excited oscillations *Wind Struc.* **7**(4):251-264.

[14] van der Pol B. (1920) A theory of the amplitude of free and forced triode vibrations, *Radio Review* **1**:701-710, 754-762.

[15] Guckenheimer J., Holmes P. (1983) Nonlinear Oscillations, Dynamical Systems and Bifurcations of Vectors Fields, Springer-Verlag, NY.

[16] Nayfeh A.H., Balachandran B. (1995) Applied Nonlinear Dynamics, Wiley, New York.

[17] Kuznetsov, Yu.A. (1998) Elements of Applied Bifurcation Theory. Springer, New York.